AIAA 81-1334R

Dynamics and Control of a Heavy Lift Airship Hovering in a Turbulent Cross Wind

B.L. Nagabhushan* and N.P. Tomlinson†
Goodyear Aerospace Corporation, Akron, Ohio

Dynamics and control characteristics of a quadrotor heavy lift airship with a sling load are determined while the vehicle is hovering in a turbulent cross wind. Results are presented which show the significance of the dynamic coupling between the vehicle and payload in their response to wind disturbances and control inputs. Typical characteristics of a closed-loop control system and its ability to limit the excursions of the vehicle and payload during loading or unloading are also examined.

Nomenclature

A, B = system dynamics matrices
C = system control matrix
F = feedback gain matrix
f_v = feedback gain proportional to vehicle velocity
f_y = feedback gain proportional to vehicle displacement
f_{v_p} = feedback gain proportional to payload velocity
f_{y_p} = feedback gain proportional to payload displacement
g = acceleration due to gravity, ft/s²
K = sling load aerodynamic drag constant (drag $= KV_p^2$)
L = scale of turbulence, ft
l = length of the payload suspension cable, ft
m_v = mass of the vehicle, slug
m_p = mass of the payload, slug
S = static lift, lb
T = disturbance matrix
u = control variable
V_m = mean wind velocity, ft/s
V_p = total velocity of the sling load, ft/s
v = lateral velocity of the vehicle along its y body axis, ft/s
v_g = turbulence velocity, ft/s
v_p = lateral velocity of the payload relative to the vehicle along the y body axis of the vehicle, ft/s
W_v = gross weight of the vehicle, lb
W_p = gross weight of the sling load, lb
$\bar{x}$ = state vector
$\dot{\bar{x}}$ = derivative of the state vector with respect to time
$Y_{A_{1s}}$ = lateral control force derivative, lb/rad
Y_v = vehicle lateral aerodynamic force derivative with respect to its lateral velocity, lb/ft/s
$Y_{\dot{v}}$ = vehicle lateral aerodynamic force derivative with respect to its lateral acceleration, slug
y = lateral displacement of the vehicle along its y body axis, ft
y_p = lateral displacement of the payload relative to the vehicle along the y body axis of the vehicle, ft
y_{p_i} = lateral displacement of the payload relative to the ground, ft
Δ = prefix used for small perturbation
ζ = damping ratio
σ = root mean square value of fluctuating wind velocity in the y direction of vehicle body axes, ft/s
ϕ_{v_g} = power spectrum of wind turbulence, ft³/s²
ω = circular frequency, rad/s
ω_n = natural frequency, rad/s
Ω = spatial frequency ($=\omega/V$), rad/ft

Presented as Paper 81-1334 at the AIAA Lighter-Than-Air Systems Conference, Annapolis, Md., July 8-10, 1981; submitted July 21, 1981; revision received Jan. 20, 1982.

*Engineer Specialist, Weapon Systems Department, Defense Systems Division. Member AIAA.
†Engineer Specialist, Computer Applications Department, Defense System Division.

Introduction

A NEW generation of vertical takeoff and landing vehicle concepts, particularly rotorcraft with unprecedented lifting capability, is being developed[1] to airlift payloads externally on a sling. The heavy-lift airship (HLA) concept belongs to this class of aircraft and offers the possibility of greatly improved low-speed controllability and stationkeeping characteristics far beyond that of historical lighter-than-air (LTA) vehicles. This concept is now being considered for various military and civil applications[2] where externally suspended payloads are transported over short distances, such as in off-loading container ships, logging, or moving construction equipment.

The HLA configuration considered in this study consists of a buoyant hull with an empennage and four interchangeable rotor modules, each consisting of a lifting rotor and an auxiliary propeller. To utilize fully the potential of this concept and also insure that the vehicle and payload motions in the operational flight regime are stable and safe, Goodyear has been investigating[3] the flight dynamics and control of such a configuration. Consequently, it has been found that a rather critical control problem would occur while the vehicle is loading and unloading its payload in the presence of atmospheric disturbances, such as a turbulent cross wind. In this paper such operational flight conditions are examined to gain insight into the dynamics and control characteristics of the vehicle/payload system. Similar studies[4] have been conducted in the past on the Aerocrane hybrid heavy lift vehicle concept.

Mathematical models describing the combined motion as well as decoupled motions of the vehicle and payload are used to determine the dynamics and control characteristics of the vehicle alone and while it is carrying a suspended payload. Further, the results predicted by the decoupled model of the payload are compared with those of the coupled model to determine the effect of motion of the payload suspension point on the payload dynamics. Subsequently, a closed-loop control system is used to examine the desirable characteristics of such a system in limiting the response of the vehicle, with or without a suspended payload, to a turbulent cross wind.

HLA/Payload Mathematical Model

Nonlinear equations of motion of the HLA carrying a simply suspended payload have been derived[5] by considering a simple model of such a configuration and are used here. Briefly, in this model the envelope is assumed to be a rigid body from which a payload, modeled as a point mass, is suspended from an arbitrary point on the vehicle by means of a rigid, nonextensible link. The rotor modules in the configuration are assumed to be rigidly connected to the hard structure and are implicit devices that produce forces and moments on the vehicle for a specified flight path of the HLA and control inputs. In the present study only the lateral dynamics of the vehicle/payload system is considered. Consequently, the relevant motions are described by translational velocity of the vehicle v along its y body axis (Fig. 1). Payload motion relative to the vehicle is described in terms of its coordinate y_p, which is defined in the reference body axes system of the vehicle. The external forces that are considered to be acting on the vehicle are due to gravity, buoyancy, aerodynamics of the envelope, tension in the payload suspension cable, and control inputs. Forces on the payload are due to gravity, aerodynamic drag, and a force equal and opposite to tension in the cable.

For the present study it is convenient to linearize these nonlinear equations about a mean wind condition corresponding to hovering in a turbulent cross wind. The resulting perturbation equations describe the vehicle and payload motion due to the turbulence velocity of a cross wind. These equations are rearranged in the state variable form

$$A\dot{\bar{x}} = B\bar{x} + Cu + Tv_g$$

where the state vector $\bar{x}^T = [\Delta v \Delta y \Delta v_p \Delta y_p \Delta y_{pi}]$ consists of perturbations in vehicle and payload state variables. Note that an additional variable y_{pi} has been introduced for convenience in determining absolute motion of the payload with reference to an inertial coordinate system which is fixed to the ground. u is the perturbation in lateral control input which corresponds to combined lateral cyclic pitch angle of all the lifting rotors. v_g is the turbulence velocity of the cross-wind disturbance. The corresponding system definition matrices are

$$A = \begin{bmatrix} m_v + m_p - Y_{\dot{v}} & 0 & m_p & 0 & 0 \\ 0 & 1 & 0 & 0 & 0 \\ m_p & 0 & m_p & 0 & 0 \\ 0 & 0 & 0 & 1 & 0 \\ 0 & 0 & 0 & 0 & 1 \end{bmatrix}$$

$$B = \begin{bmatrix} -2KV_m + Y_v & 0 & -2KV_m & 0 & 0 \\ 1 & 0 & 0 & 0 & 0 \\ -2KV_m & 0 & -3KV_m & -m_p g/l & 0 \\ 0 & 0 & 1 & 0 & 0 \\ 1 & 0 & 1 & 0 & 0 \end{bmatrix}$$

$$C = \begin{bmatrix} Y_{A_{1s}} \\ 0 \\ 0 \\ 0 \\ 0 \end{bmatrix}, \quad T = \begin{bmatrix} 2KV_m - Y_v \\ 0 \\ 3KV_m \\ 0 \\ 0 \end{bmatrix}$$

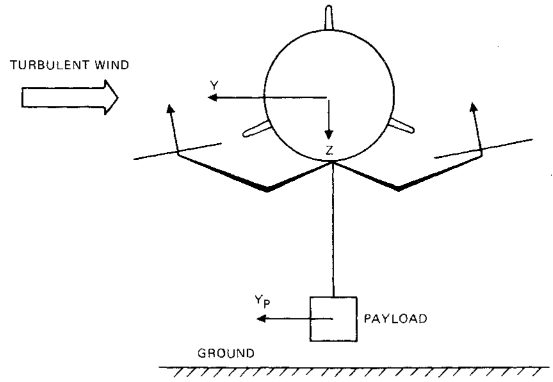

Fig. 1 HLA with sling load in cross-wind hover.

Provisions for feeding back control proportional to both the displacement and velocity of the vehicle and payload have been made by closing the loop via the control law

$$u = F\bar{x}$$

where the gain matrix

$$F = [\,-f_v \; -f_y \; -f_{v_p} \; -f_{y_p}\,]$$

It is to be noted that when the vehicle and payload motions are decoupled, the above fourth-order dynamics model reduces to two second-order dynamics models, each of which is analogous to a mechanical spring-mass-damper system. These will be discussed subsequently. The analytical techniques used in examining stability and determining response to turbulence inputs from the above linear system models can be found in the literature[6] and hence are not discussed here.

Atmospheric Disturbance Model

The capabilities of the HLA to perform under adverse weather conditions would depend upon the adequacy of its control for satisfactory operation. In order to define such a control system and perhaps the operational limits of the vehicle itself, it is necessary to characterize the operational flight conditions by representative weather scenarios through measurements or modeling of the atmosphere. Goodyear has identified several mission profiles and geographic regions of interest for HLA operation and has obtained[7] typical atmospheric conditions that are critical to the performance of the vehicle. With relevance to the present study, a weather scenario found to be critical for hovering will be used. Basically it represents an unstable atmosphere at an altitude of 656 ft with a geostrophic mean wind component of 10 knots and turbulence velocity of the fluctuations about the mean wind of 4.78 ft/s. It is assumed that the von Kármán model satisfactorily describes the corresponding power spectrum

$$\phi_{v_g}(\Omega) = \frac{2\sigma^2 L}{\pi} \frac{1}{[1 + (1.339L\Omega)^2]^{5/6}}$$

and that Gaussian probability distribution for the atmospheric turbulence is adequate. A function of this power spectrum which reflects the distribution of turbulent energy in the wind is shown in Fig. 2. Here the peak value of the function has been normalized with respect to the ordinate scale factor. It is observed that the peak frequency of the spectra is 0.014 rad/s with a corresponding wavelength of 7725 ft. Consequently, it is to be noted that the level of excitation impressed upon the HLA/payload system would depend upon the relative closeness of the system natural frequencies to this peak frequency.

In order to assess the vehicle/payload system sensitivity to atmospheric disturbances, the turbulence scale length is arbitrarily varied while keeping other quantities describing the atmospheric conditions fixed. This essentially shifts the peak frequency to a higher value for shorter scale lengths.

HLA Response to Disturbance

Consider the vehicle by itself hovering in the cross wind described previously in Fig. 2. Its aerodynamic drag resulting from the 10 knot mean wind requires a lateral control force of 7140 lb for trim. With the controls fixed at the corresponding values, the vehicle inherently has no restoring force but has damping due to aerodynamic drag. Consequently, the response of the vehicle can be characterized by its time constant, which is the amount of time the vehicle takes in reaching 63% of the asymptotic value of the velocity in responding to a disturbance. For typical physical and aerodynamic data (Table 1) the vehicle time constant in responding to the above cross-wind disturbance is found to be 10 s. If it is desired to hold position relative to ground, then a restoring force has to be generated by the control system with appropriate feedback gain proportional to the vehicle displacement. For typical values of such a gain the resulting root mean square (rms) values of vehicle lateral displacement is shown in Fig. 3. The increase in the rms value of the control force corresponds to increasing the gain proportional to vehicle rms velocity, which would augment the inherent damping of the vehicle and reduce its time constant. In the case where $f_y = 0.11$ the highest value of the rms of control force shown corresponds to a damping ratio of approximately 0.6, which resulted from a velocity gain $f_v = 0.21$. The corresponding lowest value indicates a damping ratio of 0.1 with no gain on velocity feedback.

It is found that as the scale length of the cross-wind turbulence decreases, approaching the order of vehicle geometry, the response of the vehicle increases for a given closed-loop control system. Further, larger control force is required at shorter turbulence scale lengths to maintain the same level of vehicle response (Fig. 4). The increase in rms of control force shown here was consequent to increase in velocity feedback gain, as noted before. For both values of turbulence scale the lowest value of rms of control force corresponds to the inherent damping ratio of 0.17 with no gain on velocity feedback. For the larger turbulence scale, the maximum value of control force shown represents a damping ratio of 0.67 with $f_v = 0.13$. Similarly, for the smaller turbulence scale the maximum control force shown resulted in a damping ratio of 0.57 with $f_v = 0.10$. The vehicle excursions are found to increase with increasing turbulence velocity (Fig. 5).

HLA/Payload System Response to Disturbance

The lateral motion of the HLA with a payload following a disturbance in its equilibrium flight, corresponding to hovering in a cross wind, is described by the mathematical model considered earlier. For nominal operational flight condition in which the vehicle is hovering with a 75 ton payload at the end of a 500 ft cable, the dynamics of the system is characterized by the eigenvalues of the corresponding system matrix which are referred to as modes. They consist of a stable oscillation ($\omega_n = 0.29$ rad/s, $\zeta = 0.05$) of the HLA displacement and velocity about 160 deg out of phase with those of the payload and a convergence of the displacement of the two bodies. A zero eigenvalue indicating rigid body type of displacement of the vehicle and payload is also one of the modes. It is observed that the increasing mass of the payload tends to decrease the time to half amplitude of the oscillatory mode (Fig. 6). In this case the system natural frequency remained nearly constant while the damping ratio of the oscillation has been found to increase for heavier payloads. Increasing length of the suspension cable tends to decrease the natural frequency and increase the damping ratio of the oscillatory mode (Fig. 7).

It is advantageous from an operational point of view to use a longer cable, as it allows a greater margin of error for the vehicle before producing an upsetting moment on the payload preceding its pickup. Increasing mean wind velocity up to 30 knots was found to have no significant effect on the system modes. It is important to note that in responding to a given disturbance such as control inputs and wind turbulence, the above characteristic behavior of the vehicle and payload are implicitly brought into play.

Consider the vehicle/payload system hovering in the cross wind described earlier. With the controls fixed (open loop),

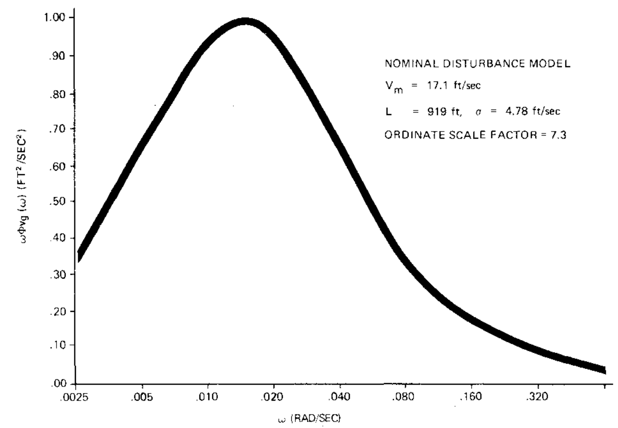

Fig. 2 Power spectrum of the wind turbulence.

Table 1 Physical and aerodynamic data for HLA/sling load configuration

W_v	= 181,314 lb
W_p	= 150,000 lb
S	= 140,807 lb
l	= 500 ft (nominal)
K	= 0.2
$Y_{\dot{v}}$	= −5975.4 slug
Y_v	= −1252.7 lb/ft/s (without payload)
	= −1361.1 lb/ft/s (with nominal payload)
$Y_{A_{ls}}$	= 29,064 lb/rad (without payload)
	= 195,144 lb/rad (with nominal payload)

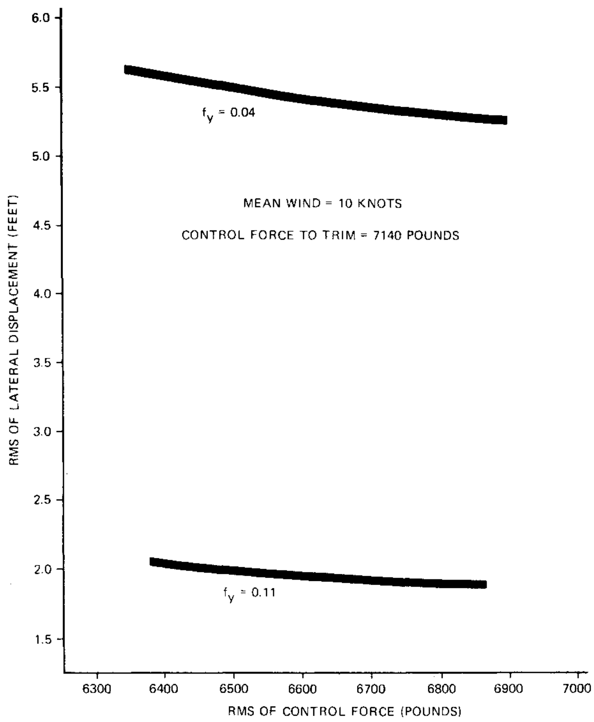

Fig. 3 Closed-loop control of HLA alone.

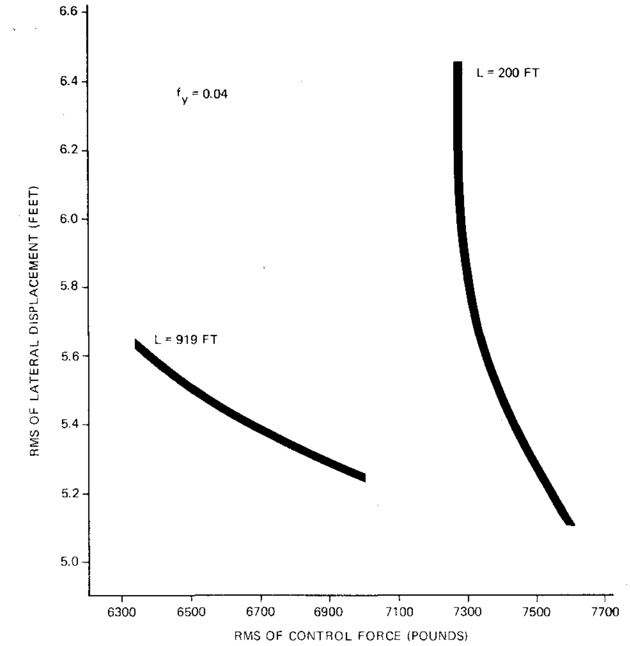

Fig. 4 Effect of varying turbulence scale on HLA response.

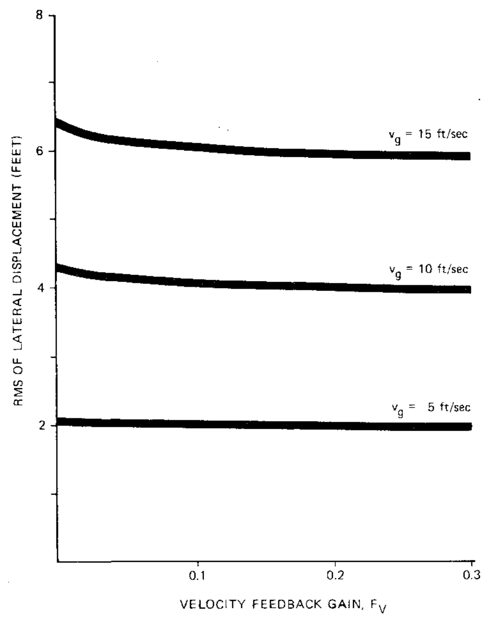

Fig. 5 Effect of varying turbulence velocity on HLA closed-loop response ($f_y = 0.11$).

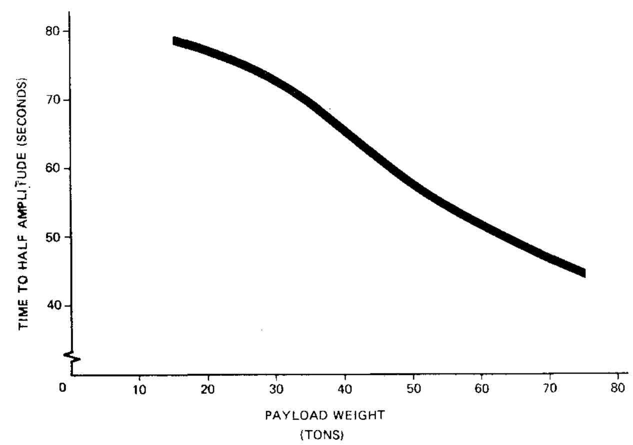

Fig. 6 Effect of varying sling load weight on system oscillatory mode ($l = 100$ ft).

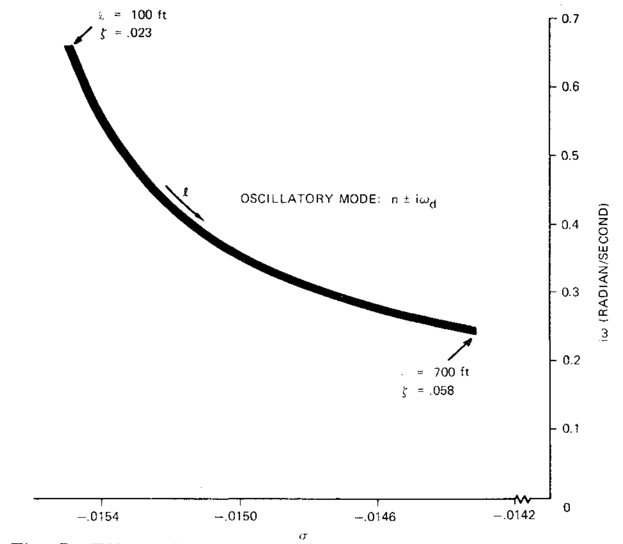

Fig. 7 Effect of varying length of payload suspension cable on system oscillatory mode.

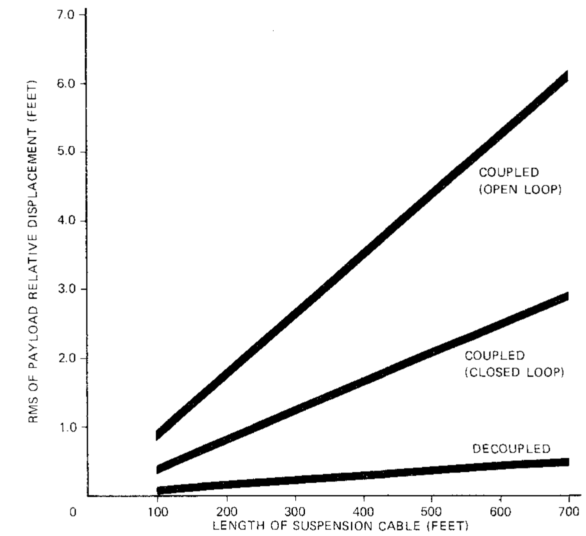

Fig. 8 Effect of varying length of payload suspension cable on rms of payload relative displacement (closed-loop gains: $f_y = 0.027$, $f_v = 0.027$).

the vehicle and payload tend to drift relative to the ground. Figure 8 shows the corresponding rms value of payload displacement relative to the vehicle for various suspension cable lengths. Comparing these results with similar data obtained by considering the decoupled payload dynamics model, which represents the payload as suspended from a fixed point and driven by wind, it is observed that the latter model tends to underpredict the payload relative motion. This also indicates that the motion of the payload suspension point should be included in predicting payload response to disturbance. It is found that increasing the turbulence scale tends to increase the rms of HLA velocity while it decreases the rms of payload velocity relative to the vehicle (Fig. 9) as well as its displacement (Fig. 10).

In order to assess the stationkeeping ability of the vehicle while it is carrying a suspended payload, a closed-loop control system similar to that considered earlier is engaged. It is found that feeding back gains proportional to the displacement and velocity of the vehicle leads to significant reduction in the relative motion (Fig. 8) of the payload as well. Figure 11 shows the resulting rms displacements of the vehicle and payload relative to the ground. The corresponding modes of the system consist of an additional oscillatory mode which is well damped and strongly coupled in the vehicle and

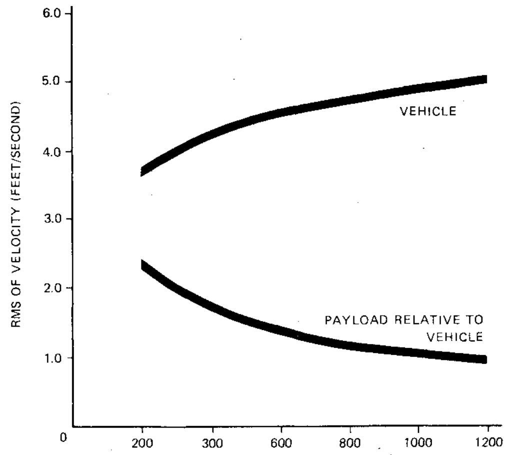

Fig. 9 Effect of varying turbulence scale on rms of HLA and payload velocity (open-loop response).

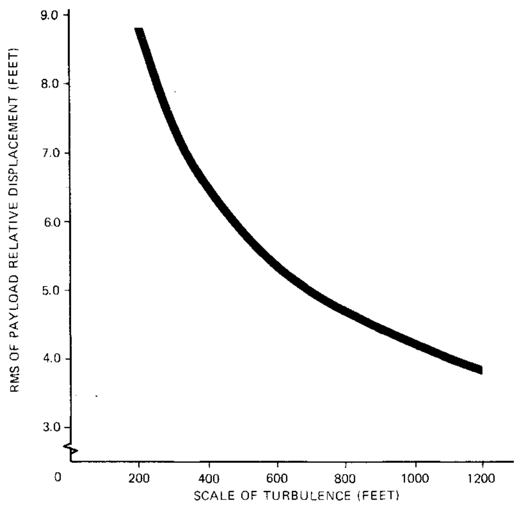

Fig. 10 Effect of varying turbulence scale on rms of payload relative displacement (open-loop response).

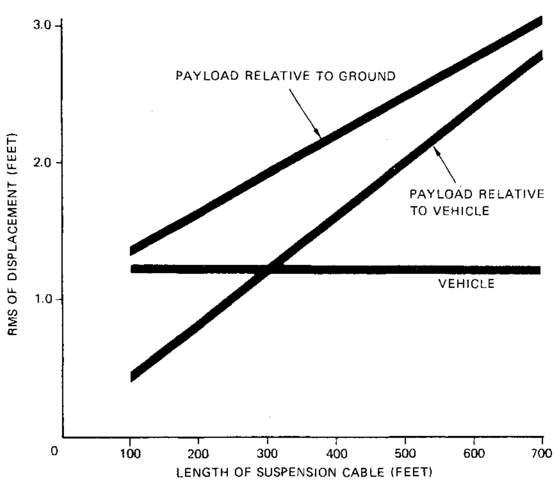

Fig. 11 Effect of varying length of payload suspension cable on rms of HLA and payload displacements (closed-loop gains: $f_y = 0.027$, $f_v = 0.027$).

payload motion. Comparing the performance of the same control system while the vehicle alone is keeping station, it is observed that tighter control, or higher gains, is required when the vehicle is hovering by itself than when it is carrying a payload to achieve the same level of response. Further, feeding back additional gains proportional to relative displacement and velocity of the payload tends to augment the system stability but not necessarily decrease the payload displacement relative to the ground. It is found that while stabilizing the combined motion of the vehicle and payload one tends to induce large displacement of the vehicle itself, leading to larger payload displacement relative to the ground. This situation could perhaps be corrected by considering a detailed design of this control system.

It is observed that the performance of a given closed-loop control system depends on the presence of the suspended payload as well as the length of the suspension cable (Fig. 11). It is found that a control system designed for operation with longer cable performs better at shorter cable lengths in limiting the payload response to wind disturbances. From an operational point of view a variable gain control system might, perhaps, be more effective and desirable.

Conclusion

The problem of controlling the HLA alone while it is hovering over a point on the ground in a turbulent cross wind is different from that of the HLA with a sling load. In the latter case, it is intended to control the payload motion indirectly or directly, such that the payload excursions relative to the ground is minimal rather than that of the vehicle. Albeit one can damp the motion of the payload relative to the vehicle via closed-loop control, it may not lead to adequate control of the payload during ground handling. It has been found that a tighter control is required to hold the position of the vehicle by itself than when it is carrying a slung payload. Dynamics of the payload suspension point on the vehicle is significant in predicting the response of the payload to disturbances. The length of the suspension cable is an important parameter in determining the extent of dynamic coupling between the vehicle and payload as well as in designing a closed-loop control system for improved vehicle performance. The system response to atmospheric turbulence increases as the turbulence scale approaches the order of vehicle/payload configuration geometry.

Further studies should consider a power spectrum of the wind turbulence model that includes wind acceleration contribution as well. This may be of special significance to this vehicle because of its buoyant characteristics. They should look into the effects of cross coupling with other lateral and directional dynamics on the system response to a cross wind. The corresponding model for wind disturbance should include correlated wind turbulence components in all of the rigid body degrees of freedom of the vehicle. A detailed design of the closed-loop control system for this vehicle would perhaps be a challenging task.

Acknowledgment

This work was performed under Goodyear Aerospace Independent Research and Development Program.

References

[1] Williams, D.E., "The Development of a Heavy Lift Airship," AHS Paper 80-9, Washington, D.C., May 1980.

[2] Mettam, P.J., Hansen, D., Byrne, R.W., and Ardema, M.D. "A Study of Civil Markets for Heavy Lift Airships," AIAA Paper 79-1579, July 1979.

[3] Nagabhushan, B.L. and Tomlinson, N.P., "Flight Dynamics Simulation of a Heavy Lift Airship," *Journal of Aircraft*, Vol. 18 Feb. 1981, pp. 96-102.

[4] Curtiss, H.C. Jr. and Putnam, W.F., "Stability and Control Characteristics of the Aerocrane Hybrid Heavy Lift Vehicle," *Journal of Aircraft*, Vol. 17, Oct. 1980, pp. 719-726.

[5] Nagabhushan, B.L., "Equations of Motion of Heavy Lift Airship with a Simply Suspended Payload," Goodyear Aerospace Corp. Rept. GER-16443, March 1977.

[6] Etkin, B., *Dynamics of Atmospheric Flight*, John Wiley & Sons New York, 1972, pp. 8-104.

[7] Williamson, G.G., "Atmospheric Turbulence Modeling Applicable to the Heavy Lift Airship," ARAP Rept. 379, Dec. 1978.